

Benzoxazines with tolyl, *p*-hydroxyphenyl or *p*-carboxyphenyl linkage and the structure–property relationship of resulting thermosets

Ching Hsuan Lin^{a,*}, Hong Tze Lin^a, Sheng Lung Chang^a, Hann Jang Hwang^b, Yu Ming Hu^a, Ya Ru Taso^a, Wen Chiung Su^c

^a Department of Chemical Engineering, National Chung Hsing University, 250, Kuo Kuang Road, Taichung 402, Taiwan

^b Department of Cosmetic Science, Chung Hwa University of Medical Technology, Tainan, Taiwan

^c Chung Shan Institute of Science and Technology, Lungtan, Taoyuan, Taiwan

ARTICLE INFO

Article history:

Received 9 July 2008

Received in revised form

20 January 2009

Accepted 26 February 2009

Available online 6 March 2009

Keywords:

Benzoxazine
Flame retardancy
Thermoset

ABSTRACT

Three benzoxazines (**7–9**) with a tolyl, *p*-hydroxyphenyl or *p*-carboxyphenyl structure, respectively, were successfully synthesized by a three-pot or two-pot procedure. In the three-pot approach, the first step is the condensation of 2-hydroxybenzaldehyde with *p*-toluidine, 4-aminophenol and 4-aminobenzoic acid, respectively, forming intermediates (**1–3**) with an imine linkage. The second step is the addition of 9,10-dihydro-9-oxa-10-phosphaphenanthrene 10-oxide (DOPO) on the imine linkage, resulting in intermediates (**4–6**) with a secondary amine linkage. The last step is the ring closure condensation of (**4–6**), leading to benzoxazines (**7–9**). In the simplified two-pot approach, the first two steps—the condensation and imine reduction were carried out in one reactor, so the yield of (**4–6**) was increased. The structures of monomers (**1–9**) were characterized and confirmed by 1D and 2D NMR spectra. The synthesized benzoxazines were thermally self-cured or copolymerized with a commercial benzoxazine, bis(3-phenyl-3,4-dihydro-2*H*-benzo[e][1,3]oxazin-6-yl)methane (**F-a**). IR analysis was utilized to monitor the ring-opening reaction of (**7–9**) and to propose the structures of P(**7–9**). The microstructure and the structure–property relationship of the resulting homopolymers and copolymers are studied.

© 2009 Elsevier Ltd. All rights reserved.

1. Introduction

Because of wide applications in electronic industries, such as printed circuit board or encapsulation, the demand of flame retardant polymers is high. To enhance the flame retardancy, some flame-retardant elements, such as alkyne [1], deoxybenzoin [2] and phosphorus [3–8] have been incorporated into polymers, and promising results have been achieved. Among the polymers used for electronic applications, benzoxazine, a resin that can be polymerized to a thermoset with a phenolic-like structure by a thermally activated cationic ring-opening reaction, exhibits the potential to replace epoxy resins for electronic applications. Although carbon fiber reinforced polybenzoxazine P(B-a) shows improved flame retardancy, the flame retardancy of neat polybenzoxazines may not meet the requirements of certain electronic applications. Thus, researches on flame-retardant polybenzoxazines are interesting for electronic industries. According to the literature, most difunctional benzoxazines were synthesized

from the reaction of aromatic biphenols, monoamines and formaldehyde [9–15]. Thus, flame-retardant elements can be incorporated into benzoxazines via aromatic biphenols or monoamines to provide flame retardancy. As a result, flame-retardant benzoxazines based on a phenylphosphine oxide-containing biphenol [13], and DOPO derivatives [16,17] have been prepared. Especially, Ulrich and Franck reported a novel method of synthesizing phosphorus-containing benzoxazines with phenyl linkages, and the flame retardancy of resulting epoxy/benzoxazine thermosets has been proven. However, due to the mono-functional characteristic of the synthesized benzoxazines, T_g s of resulting thermosets were reduced [17].

Ishida et al. [18] and Espinosa et al. [19,20] revealed that the free *ortho* of phenolic OH can initiate the ring opening of oxazine. Besides, Ishida et al. [21] and Takeichi et al. [22] proposed acid can catalyze the ring opening reaction of benzoxazine. In order to discuss the structure–property relationship of poly(benzoxazine)s, three benzoxazines (**7–9**) with a tolyl, *p*-hydroxyphenyl or *p*-carboxyphenyl groups as a substituent, respectively, were synthesized. Among the benzoxazines, benzoxazine (**7**) was synthesized according to Ulrich and Franck's approach [17], while benzoxazines (**8–9**) were synthesized by extending their

* Corresponding author. Tel.: +886 4 22850180; fax: +886 4 2285 4734.
E-mail address: linch@nchu.edu.tw (C.H. Lin).

approach. In this work, a modified two-pot approach was developed to simplify Ulrich and Franck's approach, in which a three-pot approach is required. The synthesized benzoxazines were thermally self-cured or copolymerized with a commercial benzoxazine, bis(3-phenyl-3,4-dihydro-2*H*-benzo[e][1,3]oxazin-6-yl)methane (**F-a**). The properties such as glass transition temperature, coefficient of thermal expansion, thermal decomposition temperature, flame retardancy and the structure–property relationship of the resulting homopolymers or copolymers were evaluated.

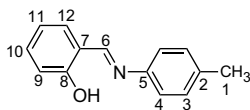
2. Experimental section

2.1. Materials

9,10-Dihydro-9-oxa-10-phosphaphenanthrene 10-oxide (DOPO) was purchased from TCI. *p*-Toluidine, 4-aminophenol and 4-amino-benzoic acid were purchased from Acros. 2-Hydroxybenzaldehyde was purchased from Showa. Bis(3-phenyl-3,4-dihydro-2*H*-benzo[e][1,3]oxazin-6-yl)methane (**F-a**) was kindly supplied by the Shikoku Chemicals Corporation, Japan. *N,N*-Dimethyl formamide (DMF) and tetrahydrofuran (THF) were purchased from Tedia and purified by distillation under reduced pressure over calcium hydride (Acros) and stored over molecular sieves. The other solvents used are commercial products (high-performance-liquid-chromatography grade) and used without further purification.

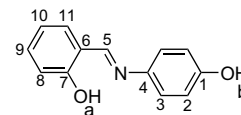
2.2. Preparation of 4-(2'-hydroxybenzylideneimino)toluene (**1**)

p-Toluidine 21.43 g (0.20 mol), 2-hydroxybenzaldehyde 24.424 g (0.20 mol), and 200 mL ethanol were introduced into a round 500 mL glass flask equipped with a nitrogen inlet, a condenser, and a magnetic stirrer. The reaction mixture was stirred at room temperature for 1.5 h. The yellow precipitate was filtered and washed twice with ethanol, and then dried at 80 °C in a vacuum oven. Yellow crystal 36.86 g (87% yield) with a melting point of 96.0 °C (DSC) was obtained. IR absorption: C–H 2922 cm⁻¹, C=N 1620 cm⁻¹. ¹H NMR (ppm, DMSO-*d*₆), δ = 2.32 (3H, H¹), 6.95 (1H, H¹¹), 6.96 (1H, H⁹), 7.25 (2H, H²), 7.32 (2H, H⁴), 7.41 (1H, H¹⁰), 7.62 (1H, H¹²), 8.93 (1H, H⁶) 13.43 (1H, OH). ¹³C NMR (DMSO-*d*₆), δ = 20.56 (C¹), 116.51 (C¹¹), 119.01 (C⁹), 119.27 (C⁷), 121.16 (C⁴), 129.88 (C³), 132.43 (C¹²), 132.98 (C¹⁰), 136.45 (C²), 145.34 (C⁵), 160.27 (C⁶), 162.48 (C⁸).



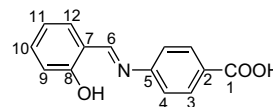
2.3. Preparation of 4-(2'-hydroxybenzylideneimino)phenol (**2**)

Compound (**2**) was prepared in a similar synthetic procedure of (**1**) using 4-aminophenol and 2-hydroxybenzaldehyde as starting material. Light orange crystal (83% yield) with a melting point of 141 °C (DSC) was obtained. IR absorption: OH 3226 cm⁻¹. C=N 1620 cm⁻¹. Mass spectrum: 214 (M+1⁺). Elemental analysis of C₁₃H₁₁O₂N: Calculated: C, 73.23%; H, 5.20%. N, 6.57%. Found: C, 73.03%; H, 5.06%; N, 6.56%. ¹H NMR (ppm, DMSO-*d*₆), δ = 6.85 (2H, H²), 6.94 (2H, H⁸ and H¹⁰), 7.32 (2H, H³), 7.37 (1H, H⁹), 7.58 (1H, H¹¹), 8.89 (1H, H⁵), 9.69 (1H, OH^b), 13.41 (1H, OH^a). ¹³C NMR (DMSO-*d*₆), δ = 115.97 (C²), 116.46 (C⁸), 118.98 (C⁶), 119.44 (C¹⁰), 122.65 (C³), 132.20 (C¹¹), 132.52 (C⁹), 139.21 (C⁴), 156.96 (C¹), 160.15 (C⁵), 160.19 (C⁷).



2.4. Preparation of 4-(2'-hydroxybenzylideneimino)benzoic acid (**3**)

Compound (**3**) was prepared in a similar synthetic procedure of (**1**) using 4-aminobenzoic acid and 2-hydroxybenzaldehyde as starting material. Yellow crystal (96% yield) with a melting point 273.3 °C (DSC) was obtained. IR absorption: C=O 1685 cm⁻¹, C=N 1625 cm⁻¹. ¹H NMR (ppm, DMSO-*d*₆), δ = 7.01 (2H, H⁹ and H¹¹), 7.53 (3H, H⁴ and H¹²), 7.66 (1H, H¹⁰), 7.95 (2H, H³), 8.98 (1H, H⁶) 12.72 (1H, OH), 12.98 (1H, COOH).

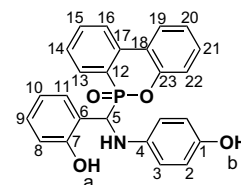


2.5. Preparation of 2-((4-methylphenylimino)(6-oxido-6*H*-dibenzoc,e)-oxaphosphorin-6-yl)methylphenol (**4**)

DOPO 21.617 g (0.1 mol), (**1**) 21.32 g (0.1 mol) and ethanol 200 mL were introduced into a round 500 mL glass flask equipped with a nitrogen inlet, a condenser, and a magnetic stirrer. The reaction mixture was cooled to 3–5 °C and then stirred at that temperature for 10 h. After that, the reaction mixture was poured into water. The precipitate was filtered and washed by water, and then dried in a vacuum oven. Light yellow powder 35.82 g (84% yield) was obtained. Since the phosphorus and the adjacent aliphatic carbon are both chiral centers, two diastereomers exist in (**4**). IR absorption: N–H stretching 3372 cm⁻¹, O–H 3200–3100 cm⁻¹, C–H 2928 cm⁻¹, P–Ph 1604 cm⁻¹, C–N 1275 cm⁻¹, P=O 1207 cm⁻¹. NMR characterization of (**4**) is shown in Fig. 1, and will be discussed later.

2.6. Preparation of 2-((4-hydroxyphenylimino)(6-oxido-6*H*-dibenzoc,e)-oxaphosphorin-6-yl)methylphenol (**5**) from (**2**)

Compound (**5**) was prepared in a similar synthetic procedure of (**4**) using (**2**) and DOPO as starting material. Yellow brown powder (90% yield) was obtained. IR absorption: N–H stretching 3400 cm⁻¹, O–H 3350–3000 cm⁻¹, P–Ph 1600 cm⁻¹, C–N 1280 cm⁻¹, P=O 1207 cm⁻¹. Similar to (**4**), two diastereomers exist in (**5**). ¹H NMR (ppm, DMSO-*d*₆), δ = 5.15 (H⁵), 5.31 (H^{5'}), 5.67 (NH¹), 6.02 (NH), 6.38 (H^{3'}), 6.42 (H³), 6.45 (H²), 6.52 (H^{2'}), 6.71–6.78 (H⁸, H^{8'}, H¹⁰, H^{10'}), 6.97 (H^{11'}), 6.98 (H²²), 7.05 (H¹¹), 7.16 (H^{22'}), 7.27–7.31 (H¹⁹, H^{19'}, H^{21'}), 7.34 (H^{15'}), 7.39 (H²¹), 7.44 (H^{9'}), 7.28 (H⁹), 7.56 (H¹⁵), 7.69 (H^{14'}), 7.76 (H¹⁴), 8.07–8.10 (H¹⁶, H^{16'}), 8.11–8.14 (H²⁰, H^{20'}), 8.16–8.18 (H¹³, H^{13'}), 8.43 (OH^b), 8.46 (OH^{b'}), 9.37 (OH^{a'}), 9.50 (OH^a).



2.7. Direct preparation of (**5**) by a simplified approach

4-Aminophenol 6.55 g (60 mmol), 2-hydroxybenzaldehyde 7.33 g (60 mmol), DOPO 12.97 g (60 mmol) and DMF 150 mL were

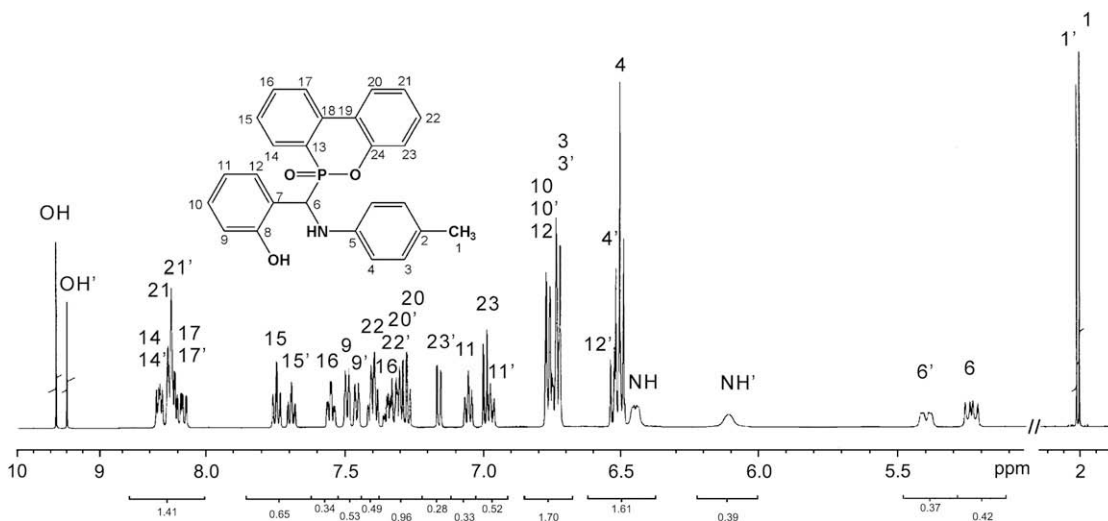
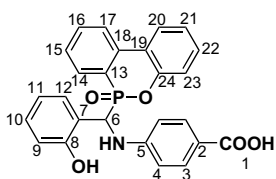


Fig. 1. ^1H NMR spectrum of (4).

introduced into a round 500 mL glass flask equipped with a nitrogen inlet, a condenser, and a magnetic stirrer. The reaction mixture was reacted at room temperature for 12 h. After that, the reaction mixture was poured into water. The precipitate was filtered and washed with water, and then dried in a vacuum oven. Light yellow powder 24.5 g (95% yield) was obtained. Compound (5) prepared by this approach has the same NMR spectrum as that prepared by the two-step procedure.

2.8. Preparation of 2-((4-carboxylic acid phenylimino)(6-oxido-6H-dibenz <c,e><1,2> oxaphosphorin-6-yl)methyl)phenol (6) from (3)

Compound (6) was prepared in a similar synthetic procedure of (4) using (3) and DOPO as starting material. Yellow powder (80% yield) was obtained. IR absorption: N–H stretching 3422 cm^{-1} , O–H $3190\text{--}3000\text{ cm}^{-1}$, C=O 1689 cm^{-1} , P–Ph 1604 cm^{-1} , C–N 1280 cm^{-1} , P=O 1200 cm^{-1} . Similar to (5), two diastereomers exist in (6). ^1H NMR (ppm, DMSO- d_6), $\delta = 5.33\text{--}5.37$ (H^6), $5.48\text{--}5.53$ ($\text{H}^{6'}$), 6.56 (H^9), 6.61 (H^4), 6.64 (H^4), 6.75 (H^{11}), 6.78 ($\text{H}^{11'}$), 6.80 (H^9), $7.00\text{--}7.02$ (H^{10} , H^{23}), 7.08 (H^{10}), 7.14 ($\text{H}^{23'}$), 7.21 (NH'), 7.27 (H^{21}), 7.32 ($\text{H}^{21'}$), 7.35 ($\text{H}^{16'}$), 7.40 (H^{22} , $\text{H}^{22'}$), 7.47 (NH), 7.49 (H^{12} , $\text{H}^{12'}$), 7.53 (H^3), 7.55 (H^{16}), 7.57 (H^3), 7.70 (H^{15}), 7.73 (H^{15}), 8.04 (H^{17}), 8.05 ($\text{H}^{17'}$), 8.11 (H^{20}), 8.12 (H^{20}), 8.14 (H^{14}), 8.16 ($\text{H}^{14'}$), 9.52 (OH^a), 9.66 (OH^a), 12.07 (H^1 , $\text{H}^{1'}$).



2.9. Direct preparation of (6) by a simplified approach

4-Aminobenzoic acid 13.71 g (0.1 mol), 2-hydroxybenzaldehyde 12.21 g (0.1 mol), DOPO 21.62 g (0.1 mol) and DMF 200 mL were introduced into a round 500 mL glass flask equipped with a nitrogen inlet, a condenser, and a magnetic stirrer. The reaction mixture was reacted at room temperature for 12 h. After that, the reaction mixture was poured into water. The precipitate was filtered and washed with water, and then dried in a vacuum oven. Light yellow powder 44.9 g (98% yield) was obtained. Compound

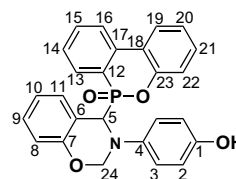
(6) prepared by this approach has the same NMR spectrum as that prepared by the two-step procedure.

2.10. Preparation of 4-(4-(6-oxido-6H-dibenz <c,e><1,2> oxaphosphorin-6-yl)-2H-benzo[1,3]oxazin-3-yl)toluene (7)

10.69 g (0.025 mol) of (4) and 100 mL of chloroform were introduced into a 500 mL round-bottom glass flask equipped with a condenser and a magnetic stirrer. 2.029 g (0.025 mol) of 37% formaldehyde in 5 mL chloroform was added. The mixture was stirred at room temperature for 6 h, and then further stirred at reflux temperature for 12 h. After that, the solvent was removed by a rotary evaporator. Off-white powder (quantitative yield) with a melting point of $154\text{ }^\circ\text{C}$ (DSC) and an exothermic peak temperature of $258\text{ }^\circ\text{C}$ was obtained. IR absorption: asymmetric Ar–O–C 1257 cm^{-1} , symmetric Ar–O–C 1036 cm^{-1} , oxazine 973 cm^{-1} . Since the phosphorus and the adjacent aliphatic carbon are both chiral centers, two diastereomers exist in (7). NMR characterization of (7) is shown in Fig. 2, and will be discussed later.

2.11. Preparation of 4-(4-(6-oxido-6H-dibenz <c,e><1,2> oxaphosphorin-6-yl)-2H-benzo[1,3]oxazin-3-yl)phenol (8)

Compound (8) was prepared in a similar synthetic procedure of (7) using (5) and 37% formaldehyde as starting material. Brown powder (quantitative yield) with two melting points of 238 and $242\text{ }^\circ\text{C}$ (DSC) and an exothermic peak temperature after $242\text{ }^\circ\text{C}$ were obtained. IR absorption: symmetric Ar–O–C 1041 cm^{-1} , oxazine 956 cm^{-1} . Similar to (7), two diastereomers exist in (8). ^1H NMR (ppm, DMSO- d_6), $\delta = 4.75\text{--}5.39$ (H^5 , $\text{H}^{5'}$, H^{24} , $\text{H}^{24'}$), $6.35\text{--}6.41$ (H^2 , $\text{H}^{2'}$, H^3 , $\text{H}^{3'}$), $6.74\text{--}6.79$ (H^8 , $\text{H}^{8'}$, H^{10}), 6.90 ($\text{H}^{10'}$), 7.00 (H^{11}), $7.08\text{--}7.12$ (H^9 , $\text{H}^{9'}$), $7.12\text{--}7.29$ ($\text{H}^{11'}$, H^{13} , $\text{H}^{13'}$, H^{15} , $\text{H}^{15'}$), 7.32 (H^{14}), 7.41 ($\text{H}^{14'}$), $7.48\text{--}7.52$ (H^{21} , $\text{H}^{21'}$), $7.71\text{--}7.76$ (H^{20} , $\text{H}^{20'}$), $7.80\text{--}7.87$ (H^{22} , $\text{H}^{22'}$), 8.11 (H^{16}), 8.13 ($\text{H}^{16'}$), 8.20 (H^{19}), 8.22 ($\text{H}^{19'}$), 9.00 (OH).



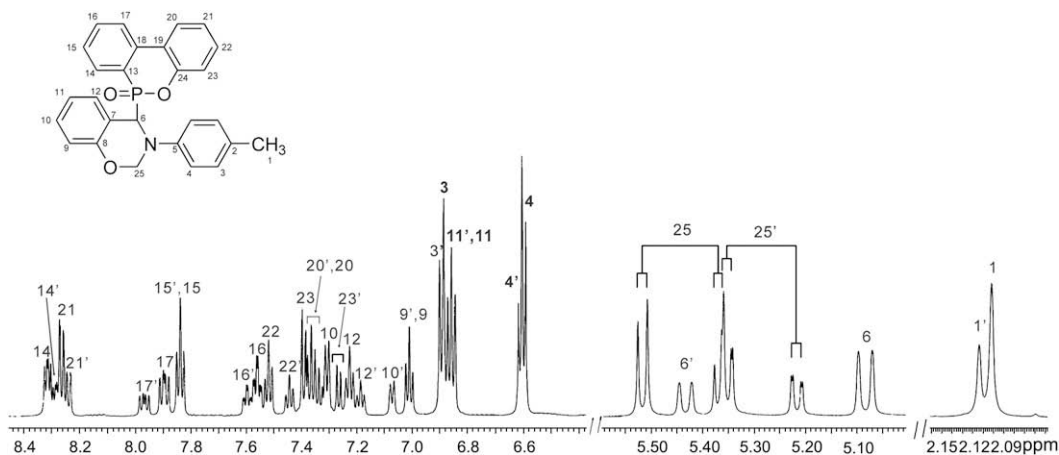
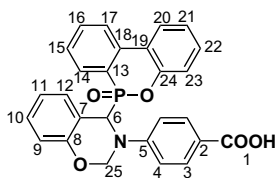


Fig. 2. ^1H NMR spectrum of (7).

2.12. Preparation of 4-(4-(6-oxido-6H-dibenz <c,e><1,2>oxaphosphorin-6-yl)-2H-benzo[1,3]oxazin-3-yl)benzoic acid (9)

Compound (9) was prepared in a similar synthetic procedure of (7) using (6) and 37% formaldehyde as starting material. White powder (quantitative yield) with a melting point of 248 °C (DSC) and an exothermic peak temperature of 268 °C was obtained. IR absorption: asymmetric Ar–O–C 1242 cm^{-1} , symmetric Ar–O–C 1037 cm^{-1} , oxazine 948 cm^{-1} . Similar to (8), two diastereomers exist in (9). ^1H NMR (ppm, DMSO- d_6), δ = 5.39 (H^6), 5.42 ($\text{H}^{6'}$), 5.56–5.86 (H^{25} , $\text{H}^{25'}$), 6.84–6.88 (H^4 , $\text{H}^{4'}$, H^9 , $\text{H}^{9'}$), 6.89 (H^{11}), 7.02 ($\text{H}^{11'}$), 7.11 (H^{12}), 7.19 (H^{10}), 7.21–7.24 ($\text{H}^{10'}$, H^{21}), 7.32–7.36 ($\text{H}^{21'}$, H^{23} , $\text{H}^{23'}$), 7.38 ($\text{H}^{12'}$), 7.48 (H^{22}), 7.47 ($\text{H}^{22'}$), 7.52 (H^{15}), 7.61 ($\text{H}^{15'}$), 7.64 (H^3), 7.68 ($\text{H}^{3'}$), 7.79 (H^{14}), 7.80–7.84 (H^{16} , $\text{H}^{16'}$), 8.01 ($\text{H}^{14'}$), 8.22 (H^{20}), 8.24–8.28 (H^{17} , $\text{H}^{20'}$), 8.32 (H^{17}), 12.56 (H^1 , $\text{H}^{1'}$).



2.13. Preparation of polybenzoxazine

Benzoxazines (7–9) were melted and stirred continuously in an aluminum mold, and then cumulative curing at 160, 180, 200 and 220 °C for 2 h each in an air-circulating oven. In addition to the homopolymerization of (7–9), (7)/F-a and (8)/F-a with various weight ratios were copolymerized in the same curing procedure. Thereafter, samples were allowed to cool slowly to room temperature to prevent cracking.

2.14. Characterization

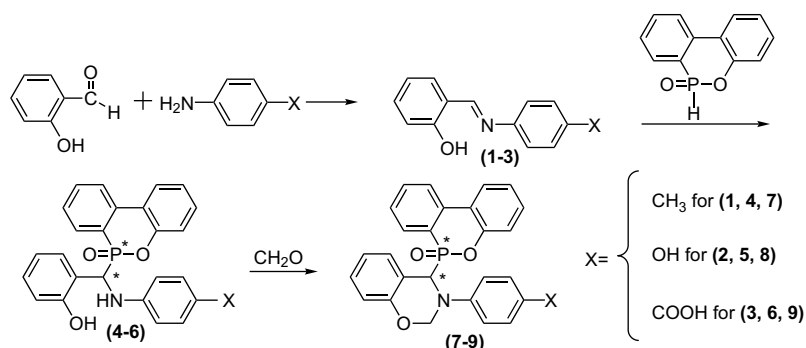
Differential scanning calorimetry (DSC) scans were obtained from samples of about 10 mg in a nitrogen atmosphere at a heating rate of 20 °C/min using a Perkin–Elmer DSC 7. T_g was taken as the midpoint of the heat capacity transition between the upper and lower points of deviation from the extrapolated liquids and glass lines. Dynamic mechanical analysis was performed with a Perkin–Elmer Pyris Diamond DMA with a sample size of $5.0 \times 1.0 \times 0.2$ cm. The storage modulus E' and $\tan \delta$ were determined as the sample was subjected to the temperature scan mode at a programmed heating rate of 5 °C/min at a frequency of 1 Hz. The test was

performed by bending mode with an amplitude of 5 μm . Thermal mechanical analysis (TMA) was performed with a Seiko TMA/SS6100 at a heating rate of 5 °C/min in a penetration mode with a constant load of 100 mN. Thermal gravimetric analysis (TGA) was performed with a Seiko Exatar 600 at a heating rate of 20 °C/min under nitrogen atmosphere from 60 °C to 800 °C. The NMR measurements were performed in DMSO- d_6 by a Varian Inova 600 NMR, and the chemical shift was calibrated by setting the chemical shift of DMSO- d_6 as 2.49 ppm. The assignment of individual peaks was assisted by the correlations shown in the ^1H – ^1H COSY and ^1H – ^{13}C HETCOR NMR spectra. The UL-94 vertical test was performed according to the testing procedure of FMVSS 302/ZSO 3975 with a test specimen bar of 127 mm in length, 12.7 mm in width and about 1.27 mm in thickness. In the test, the polymer specimen is subjected to two 10-sec ignitions. After the first ignition, the flame is removed and the time for the polymer to self-extinguish (t_1) is recorded. Cotton ignition would be noted if polymer dripping occurs during the test. After cooling, the second ignition is performed on the same sample and the self-extinguishing time (t_2) and dripping characteristics are recorded. If t_1 plus t_2 is less than 10 s without any dripping, the polymer is considered to be a V-0 material. If t_1 plus t_2 is in the range of 10–30 s without any dripping, the polymer is considered to be a V-1 material. The IR spectra were measured with a Perkin–Elmer spectrum RX1. Mass spectra were obtained using a Finnigan/Thermo QuestMAT 95XL mass spectrometer.

3. Result and discussion

3.1. Synthesis and characterization of (1–3)

As shown in Schemes 1 and 2, the imine-containing intermediates (1–3) were synthesized by the condensation of 2-hydroxy-benzaldehyde with *p*-toluidine, 4-aminobenzoic acid, and 4-aminophenol, respectively. According to the ^1H NMR data of (1–3), the aldehyde signal of 2-hydroxybenzaldehyde at 10.8 ppm disappeared, but a signal at around 8.9 ppm standing for an imine linkage appeared, supporting the formation of an imine linkage. The phenolic OH signal of 2-hydroxybenzaldehyde is at 10.20 ppm, but the phenolic OH signal of (1–3) downshifts to around 13.0 ppm. The phenolic OH–imine resonance, which lowers the electron density of phenolic OH, is responsible for the downshift of chemical shift. Besides, the intramolecular 6-membered hydrogen bonding that will reduce the electron density of phenolic OH may also contribute to the large chemical shift [23]. In the ^{13}C NMR data, the characteristic peak of imine at around 160 ppm confirms the condensation. The detailed



Scheme 1. Synthesis of benzoxazines (7–9) by a three-pot procedure.

assignment of other peaks is shown in Section 2, and it confirms the structure of (1–3).

3.2. Synthesis and characterization of (4–6)

The DOPO-containing intermediates (4–6) were synthesized by nucleophilic addition DOPO on the imine linkage of (1–3). Since the phosphorus and the adjacent aliphatic carbon are both chiral centers, four stereoisomers were resulted in each compound. Each stereocenter can be either R or S configuration, and hence, the possible combinations are RR, RS, SR, and SS configurations. The four stereoisomers can be grouped into two pairs of enantiomers, resulting in two diastereomers (RR + SS and RS + SR). In contrast with enantiomers, diastereomers, because they are not mirror images of each other, are distinct molecules with different spectroscopic data. Fig. 1 shows the ^1H NMR spectrum and the assignment of (4). As in Fig. 1, two phenolic OH peaks at 9.42 and 9.58 ppm, two methyl peaks at 2.02 and 2.04 ppm, two secondary amino peaks at 6.46 and 6.16 ppm, and two aliphatic hydrogen peaks (H^6 and $\text{H}^{6'}$) at 5.40 and 5.25 ppm confirm the existence of two diastereomers. The two phenolic OH signals upshift from 13.4 ppm to 9.4 and 9.6 ppm. The upshift is reasonable because the phenolic OH–imine resonance was destroyed after the DOPO–imine addition. Besides, the appearance of two secondary amino signals and two methylene signals confirms the DOPO–imine addition. In the ^{31}P NMR spectrum, two peaks at 37.58 and 34.21 were observed, also confirming the existence of two diastereomers.

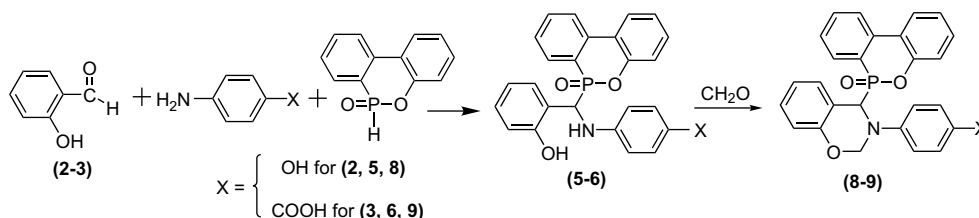
3.3. Synthesis of (5–6) by a simplified approach

The DOPO-containing intermediates (5–6) can also be synthesized by a simplified, one-pot procedure (Scheme 2). In this procedure, the first two steps—the condensation and imine reduction were carried out in one reactor. The imine linkage formed in the first stage and the DOPO–imine addition occurred in the second stage. Liu reported the nucleophilic addition of DOPO on aldehyde at high temperature [24]. However, according to the NMR spectra, the addition was successfully avoided in this

approach since the reaction temperature was kept at room temperature. The yield of (5–6) by this approach is as high as 95 and 98%, respectively. However, the total yield of (5–6) by the previous two-pot procedure is only 75% and 77%, respectively. The immediate nucleophilic addition of DOPO on the imine linkages shifts the condensation, which is a reversible one, to right, explaining the higher yield. This one-pot procedure increases the yield, and simplifies the synthetic procedure.

3.4. Synthesis and characterization of (7–9)

In the ring closure step, formaldehyde was added [25] into the solution of (4–6) to react with the secondary amine at room temperature, resulting in a presumable intermediate with a hydroxymethylamine (NCH_2OH) structure. Thereafter, the reaction temperature was raised to induce the ring closure condensation between the hydroxymethylamine and *o*-hydroxy, forming benzoxazines (7–9). This reaction can be conducted with quantitative yield in ethanol, 1,4-dioxane or chloroform at the reflux temperature of each solvent. Among the solvents, chloroform is the best solvent for this reaction because the immiscibility of chloroform with water promotes the completion of the reaction [26]. Additionally, the low boiling point of chloroform makes it easy to be removed by a rotary evaporator. Fig. 2 shows the ^1H NMR spectrum of (7). The appearance of characteristic oxazine peaks at around 5.20–5.50 ppm supports the formation of benzoxazines. Two sets of signals for methyl peaks (H^1 and $\text{H}^{1'}$), N–CH–ph (H^6 and $\text{H}^{6'}$), and N– CH_2 –O (H^{25} and $\text{H}^{25'}$) confirm the existence of two diastereomers. The peak pattern of H^{25} and $\text{H}^{25'}$ was a little complex because the H^6 is a chiral center, making the two hydrogens of H^{25} magnetically unequivalent. That is, two hydrogens will split each other with a geminal coupling. However, the peak pattern can still be interpreted in a ^1H – ^1H NMR spectrum (not shown for brevity). Two peaks at 35.5 and 32.0 were observed in the ^{31}P NMR spectrum, also confirming the existence of two diastereomers. Similar ^1H , ^{13}C NMR and ^{31}P NMR analyses were obtained for benzoxazines (8–9) (not shown for brevity), and the detailed assignment of each peak shown in Section 2 verifies their structures.



Scheme 2. Synthesis of benzoxazines (8–9) by a two-pot procedure.

3.5. DSC thermograms of benzoxazines

Fig. 3 shows the DSC thermograms of benzoxazines (7–9). Benzoxazine (7) shows a melting point at 154 °C and an exothermic peak temperature at 258 °C, demonstrating a wide processing window. Benzoxazine (8) shows two melting points at 238 and 242 °C (due to the existence of two diastereomers), and cures immediately after melting. Benzoxazine (9) shows a melting point at 248 °C, a shoulder at 252 °C, and a rapid exotherm after melting. DSC data shows that both benzoxazines display small processing window, making it difficult to become a void-free sample after curing. The free *ortho* or *para* of phenolic OH, which can initiate the ring opening of oxazine, should be responsible for the immediate curing of (8). This result is consistent with those reported by Ishida [18] and Espinosa et al. [19,20] The benzoic acid, which can catalyze the ring opening of benzoxazine, as proposed by Ishida et al. [21] and Takeichi et al. [22] explains the immediate curing of (9) after melting.

3.6. Properties of homopolymers

3.6.1. T_g and microstructure of P(7–9)

According to DSC measurement (Fig. 4), T_g s of polybenzoxazines P(7–9) are 124, 161 and 205 °C, respectively. According to the literature [27], the monofunctional benzoxazines typically lead to a linear or branched oligomer. Since benzoxazine (7) is a monofunctional monomer, P(7) is a linear or branched oligomer (Scheme 3a), therefore, exhibiting the lowest T_g . The T_g of P(7) is comparable to that of other mono-functional benzoxazines, such as poly(6-adamantyl-3-phenyl-3,4-dihydro-2H-1,3-benzoxazine) (T_g 109 °C) [28], and poly(P-a) (T_g 120 [29], 128 °C [28]). As to P(8), the free *ortho* or *para* of the phenolic OH, which can react with oxazine linkage [18–20], makes P(8) a crosslinked polymer (Scheme 3b). According to DSC data, the T_g of P(8) (161 °C) is comparable to difunctional P(F-a) [30,31]. The speculation of crosslinking can also be confirmed by the solubility test of P(7) and P(8). P(7) is soluble in organic solvents such as NMP, DMAc and DMSO, while P(8) is only slightly soluble in those solvents. In order to explain the highest T_g of P(9), IR analysis was employed. Fig. 5 shows IR spectra of (9) after accumulative curing at each stage for 20 min. After curing at 220 °C, the disappearance of Ar–O–C absorption at 1037 cm^{-1} and the oxazine absorptions at 948 and 1367 cm^{-1} indicated the ring opening of the oxazine linkage. Besides, after curing at 220 °C, the disappearance of carbonyl absorption at 1681 cm^{-1} and the appearance of ester absorptions at 1706 and 1272 cm^{-1} suggest the

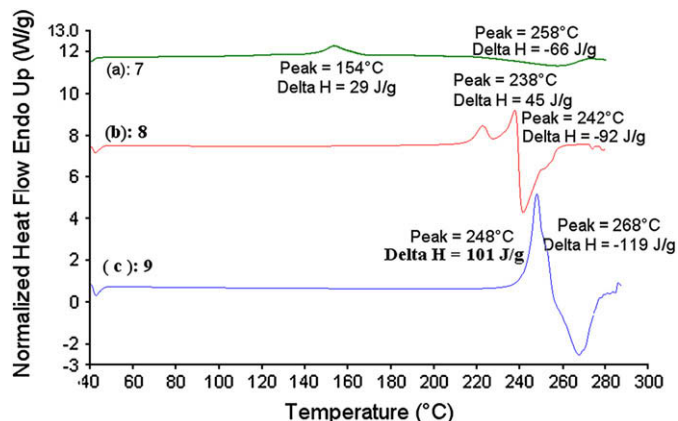


Fig. 3. DSC thermograms of benzoxazines (7–9).

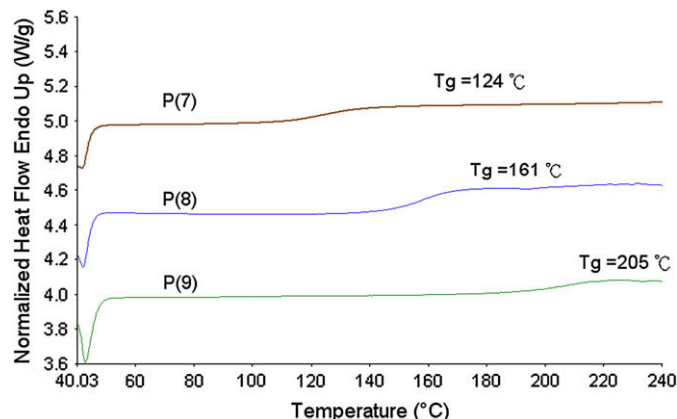


Fig. 4. DSC thermograms of polybenzoxazines P(7–9).

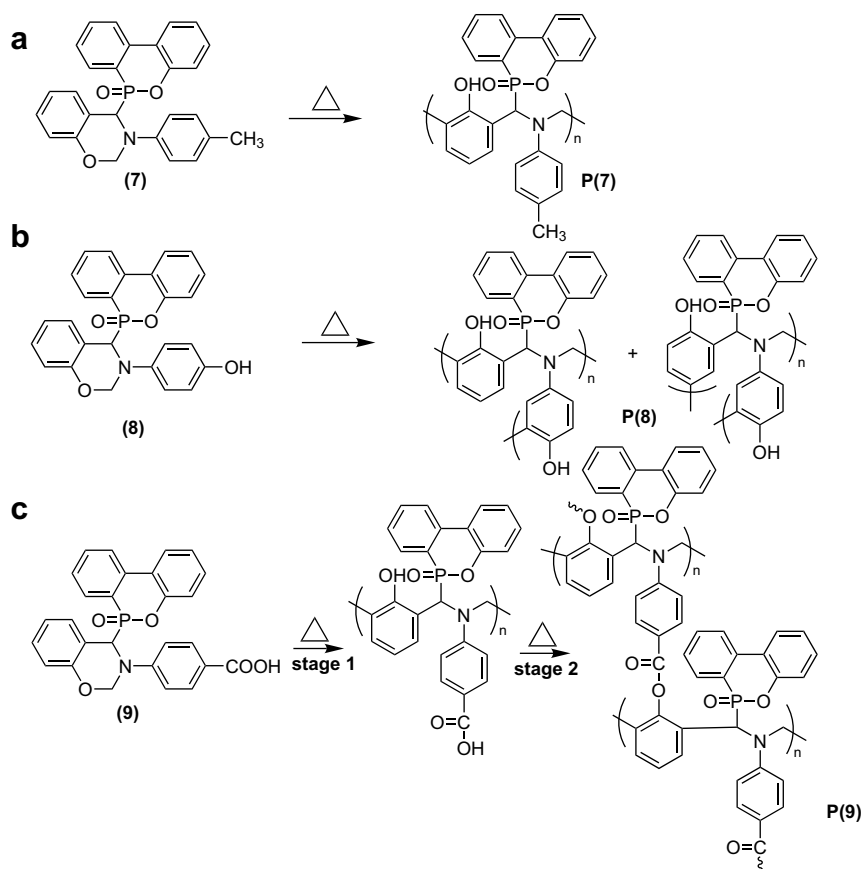
esterification of benzoic acid and phenolic OH, which is resulted from ring opening of oxazine. Similar condensation was also observed by Takeichi et al. in the poly(amic acid)–phenolic OH condensation [22]. Solubility test also show that P(9) is insoluble in organic solvents such as NMP, DMAc and DMSO, demonstrating it is a crosslinked polymer. As a result, according to the IR and DSC analyses, the structures of P(9) are shown in Scheme 3c. The esterification explains the highest T_g of P(9).

3.6.2. Thermal stability of P(7–9)

The thermal stability of the resulting polybenzoxazines was evaluated by TGA in a nitrogen atmosphere (Fig. 6). The 5% decomposition temperatures of P(7–9) are 333, 350 and 330, respectively, which are higher than that of P(F-a) (306 °C). According to the literature [32–34], the release of aniline fragment is responsible for the low thermal stability of polybenzoxazines, so the 5% degradation temperatures of common polybenzoxazines are not high. Therefore, introduction of a cross-linkable site into aniline, such as ethynyl [35–37], nitrile group [10] and propargyl ether [8], which cures at higher temperature, has been proved an effective way to enhance thermal stability of polybenzoxazines. Instead of linking to a phenyl pendant that may lead to an N–ph elimination at high temperature, the nitrogen linkage in P(7–9) is bonded to the other repeating unit, making P(7–9) thermally more stable than P(F-a). As in Fig. 6, P(8) exhibits higher thermal stability than P(7). The higher crosslinking density of P(8) and the aliphatic methyl groups of P(7) might be responsible for the phenomenon. However, the thermal stability of P(9) is not as high as P(8) although it has higher T_g . Since the esterification of benzoic acid and phenolic OH proceeded continuously at higher temperature, the continuous release of water at higher temperature reduced the 5% decomposition temperature, explaining the lower thermal stability of P(8) than P(9). In addition to lower stability, the release of water during the curing makes P(9) a porous structure, limiting its industrial application unless curing in an autoclave.

3.7. Thermal and flame-retardant properties of copolymers

In the copolymer system, benzoxazines (7–8) can dissolve into the melt of F-a, forming a void-free sample. So, the copolymers are void-free and tough enough for DMA and TMA measurement. Fig. 7 shows the DMA curves of (a)(7)/F-a and (b)(8)/F-a copolymers. T_g s decrease apparently with the content of (7) in the (7)/F-a copolymerization system, but only decrease slightly with the content of



Scheme 3. Structures of (a)P(7), (b)P(8) and (c)P(9).

(8) in the (8)/F-a copolymerization system. For example, as in Table 1, when the phosphorus content is 1.5 wt%, T_g maintains as high as 174 °C for the (8)/F-a copolymer, P(8F-1.50). However, it reduces to 159 °C for the (7)/F-a copolymer, P(7F-1.50). Similar trend was observed in the DSC and TMA measurements. As in Table 1, the dimensional stability of copolymers was improved via the small loading of (8), and the CTE of P(8F) system reached a minimum of 35 ppm/°C at the phosphorus content of 1.0 wt%. In contrast, the CTE of P(7F) system increases with the content of (7). For example,

the CTE of P(F-a) is 50 ppm/°C; however, as in Fig. 8, the CTE of P(8F-1.00) lowers to 35 ppm/°C, while the CTE of P(7F-1.00) increases to 55 ppm/°C. The DMA and TMA results suggest that incorporating *p*-hydroxyphenyl-containing (8) into F-a not only maintains high T_g s but also enhances the dimensional stability. As to the flame retardancy, thermoset with a UL-94 V-0 grade can be achieved with phosphorus content as low as 0.75 wt% for the (8)/F-a copolymers, while 1.0 wt% is required for the (7)/F-a copolymers.

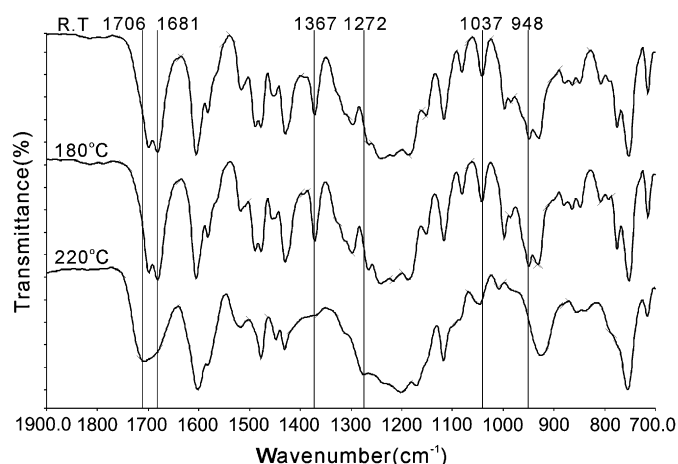


Fig. 5. IR spectra of (9) after accumulative curing at each stage for 20 min.

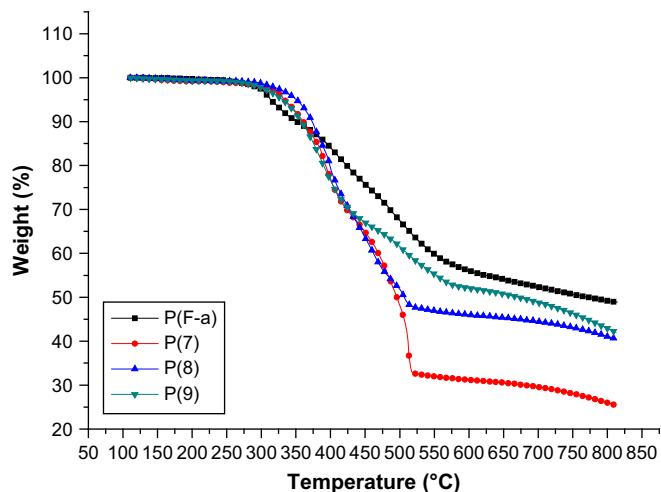


Fig. 6. TGA thermograms of polybenzoxazines P(7-9) and P(F-a).

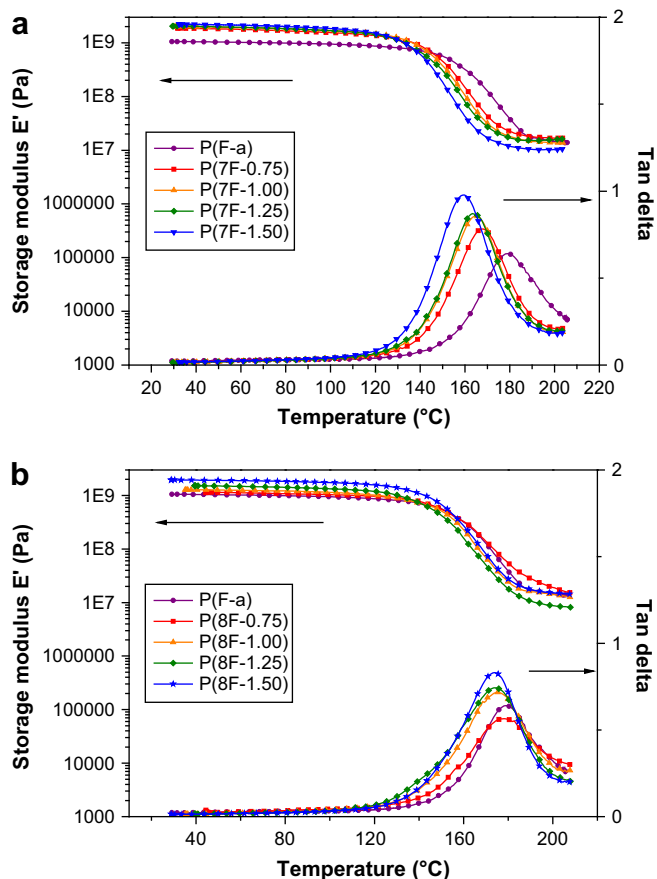


Fig. 7. DMA curves of (a) (7)/F-a and (b) (8)/F-a copolymers.

This result suggests that *p*-hydroxyphenyl-containing (**8**) exhibits better flame retardancy. As in Table 1, the T_g corresponding to a UL-94 V-0 grade in the (8)/F-a copolymerization system is as high as 178 °C, which is 13 °C higher than that in the (7)/F-a copolymerization system. Thus, incorporating *p*-hydroxyphenyl-containing (**8**) into conventional benzoxazine, such as F-a, is a better way than tolyl-containing (**7**) to improve flame retardancy and maintain thermal properties of polybenzoxazines.

Table 1
Thermal properties of (7)/F-a and (8)/F-a copolymers.

Polymer ID	Phosphorus content (wt%)	T_g^c (DMA)	T_g^d (DSC)	T_g^e (TMA)	CTE ^f	T_d^g	Char yield ^h	UL-94 Grade
P(F-a)	0	180	162	153	50	306	46	V-2
P(7F-0.75) ^a	0.75	167	156	149	51	336	45	V-1
P(7F-1.00)	1.00	165	145	144	55	327	48	V-0
P(7F-1.25)	1.25	163	143	138	61	331	43	V-0
P(7F-1.50)	1.50	159	141	134	65	322	48	V-0
P(8F-0.75) ^b	0.75	178	157	152	36	329	49	V-0
P(8F-1.00)	1.00	175	157	146	35	330	50	V-0
P(8F-1.25)	1.25	174	154	144	36	331	51	V-0
P(8F-1.50)	1.50	174	152	139	48	339	49	V-0

^a For (7)/F-a copolymers, the number after dash is the phosphorus content (wt%).

^b For (8)/F-a copolymers, the number after dash is the phosphorus content (wt%).

^c (°C) peak of tan δ , measured by DMA.

^d (°C) measured by DSC.

^e (°C) measured by TMA.

^f (ppm/°C) Coefficient of thermal expansion before T_g .

^g (°C) 5% decomposition temperature in nitrogen.

^h (wt%) residual weight percentage at 800 °C in nitrogen.

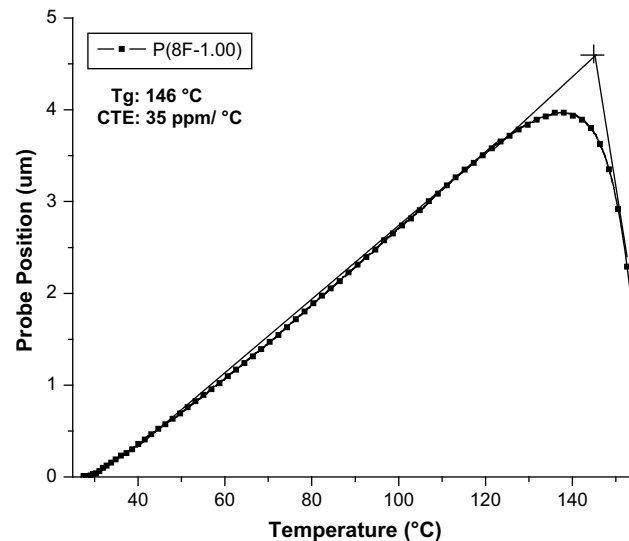


Fig. 8. TMA curve of P(8F-1.00).

4. Conclusions

New benzoxazines (**8–9**) with a *p*-hydroxyphenyl and *p*-carboxyphenyl linkage, respectively, were successfully prepared by extending Ulrich and Franck's approach. In addition, we report a modified approach to simplify the synthetic procedure of (**8–9**). The free *ortho* or *para* of the phenolic OH, which can react with other oxazine ring, justifies the higher T_g of P(**8**). The esterification between benzoic acid and phenolic OH explained the highest T_g . However, the release of water during curing makes P(**9**) a porous structure, limiting its industrial application unless curing in an autoclave. In the copolymerization system, slight decrease in T_g with the content of (**8**) was observed in the (8)/F-a system, while obvious decrease in T_g with the content of (**7**) was observed in the (7)/F-a system. Thermoset with a UL-94 V-0 grade can be achieved with a phosphorus content as low as 0.75 wt% in the (8)/F-a system, and the corresponding T_g is as high as 178 °C. Thus, incorporating *p*-hydroxyphenyl-containing (**8**) into conventional benzoxazine is a better way than tolyl-containing (**7**) to improve flame retardancy and maintain thermal properties of polybenzoxazines.

Acknowledgements

The authors thank the National Science Council of the Republic of China for financial support. Partially sponsorship by the Green Chemistry Project (NCHU), as funded by the Ministry of Education is also gratefully acknowledged.

References

- [1] Morgan AB, Tour JM. *Macromolecules* 1998;31:2857.
- [2] Ellzey KA, Ranganathan T, Zilberman J, Coughlin EB, Farris RJ, Emrick T. *Macromolecules* 2006;39:3553.
- [3] Liu YL. *J Polym Sci Part A Polym Chem* 2002;40:359.
- [4] Allcock HR, Hartle TJ, Taylor JP, Sunderland NJ. *Macromolecules* 2001;34:3896.
- [5] Lligadas G, Ronda JC, Galià M, Cádiz V. *J Polym Sci Part A Polym Chem* 2006;44:5630.
- [6] Hergenrother PM, Thompson CM, Smith Jr JG, Connell JW, Hinkley JA, Lyon RE, et al. *Polymer* 2005;46:5012.
- [7] Hoffmann T, Pospiech D, Häußler L, Komber H, Voigt D, Harnisch G, et al. *Macromol Chem Phys* 2005;206:423.
- [8] Braun U, Knoll U, Schartel B, Hoffmann T, Pospiech D, Artner J, et al. *Macromol Chem Phys* 2006;207:1501.
- [9] Agig T, Takeichi T. *Macromolecules* 2001;34:7257.
- [10] Agig T, Takeichi T. *Macromolecules* 2003;36:6010.
- [11] Brunovska Z, Ishida H. *J Appl Polym Sci* 1999;73:2937.

- [12] Ishida H, Ohba S. *Polymer* 2005;46:5588.
- [13] Choi SW, Ohba S, Brunovska Z, Hemvichian K, Ishida H. *Polym Degrad Stab* 2006;91:1166.
- [14] Kimura H, Murata Y, Matsumoto A, Hasegawa K, Ohtsuka K, Fukuda A. *J Appl Polym Sci* 1999;74:2266.
- [15] Su YC, Chang FC. *Polymer* 2003;44:7989.
- [16] Lin CH, Cai SX, Leu TS, Hwang TY, Lee HH. *J Polym Sci Part A Polym Chem* 2006;44:3454.
- [17] Ulrich W, Franck M. WO 02/057279 A1, 2002.
- [18] Ishida H, Rodriguez Y. *J Appl Polym Sci* 1995;58:1751.
- [19] Espinosa MA, Cadiz V, Galia M. *J Polym Sci Part A Polym Chem* 2004;42:279.
- [20] Espinosa MA, Cádiz V, Galia M. *J Appl Polym Sci* 2003;90:470.
- [21] Dunkers J, Ishida H. *J Polym Sci Part A Polym Chem* 1999;37:1913.
- [22] Takeichi T, Guo Y, Rimdusit S. *Polymer* 2005;46:4909.
- [23] Schnell I, Brown SP, Low HY, Ishida H, Spiess HW. *J Am Chem Soc* 1998;120:11784.
- [24] Liu YL, Wu CS, Hsu KY, Chang TC. *J Polym Sci Part A Polym Chem* 2002;40:2329.
- [25] Burke WJ. *J Am Chem Soc* 1949;71:609.
- [26] Ishida H, Low HY. *J Appl Polym Sci* 1998;69:2559.
- [27] Douglas JA, Ishida H. *Polymer* 2007;48:6763.
- [28] Su YC, Chen WC, Chang FC. *J Appl Polym Sci* 2004;94:932.
- [29] Liu YL, Yu JM. *J Polym Sci Part A Polym Chem* 2006;44:1890.
- [30] Lin CH, Chang SL, Lee HH, Chang HC, Hwang KT, Tu AP, et al. *J Polym Sci Part A Polym Chem* 2008;46:4970.
- [31] Lin CH, Chang SL, Hsieh CW, Lee HH. *Polymer* 2008;49:1220.
- [32] Kimura H, Matsumoto A, Hasegawa K, Ohtsuka K, Fukuda A. *J Appl Polym Sci* 1997;68:1903.
- [33] Ishida H, Hemvichian K. *Polymer* 2002;43:4391.
- [34] Low HY, Ishida H. *Polymer* 1999;40:4365.
- [35] Kim HJ, Brunovska Z, Ishida H. *Polymer* 1999;40:1815.
- [36] Kim HJ, Brunovska Z, Ishida H. *Polymer* 1999;40:6565.
- [37] Kim HJ, Brunovska Z, Ishida H. *J Appl Polym Sci* 1999;73:857.